JOURNAL OF THE
CHUNGCHEONG MATHEMATICAL SOCIETY
Volume **36**, No. 1, February 2023
http://dx.doi.org/10.14403/jcms.2023.36.1.25

A STUDY OF DEFECTS IN LIQUID CRYSTALS ON A PUNCTURED DISK

He Jin and Jinhae Park

Abstract. In this paper, we consider the Landau-de Gennes energy functional for liquid crystals confined in a thin cylindrical domain and study defects of molecular directions in the system by applications of external fields.

1. Introduction

In this article, we consider a nematic liquid crystal confined between two coaxial cylindrical surfaces whose internal and external radii are l and s $(0 < \ell < s)$, respectively. It is observed by numerical experiment [5] that for a sufficiently small height of the cylinder, directions of molecules are independent of the height. For this reason, in order to study behaviour of molecules in a thin cylindrical domain we only need to consider a liquid crystal in a two dimensional domain $\Omega = B_s \backslash B_\ell \subset \mathbf{R}^2$ which is a region between two concentric balls of radii s and ℓ centered at the origin.

In the Landau-de Gennes theory, a liquid crystal is described by the order tensor Q which is traceless 3×3 symmetric matrix. It can be represented as

$$Q = S_1(\mathbf{n} \otimes \mathbf{n} - \frac{1}{3}I) + S_2(\mathbf{m} \otimes \mathbf{m} - \frac{1}{3}I),$$

where S_1 and S_2 are real, and $\{\mathbf{n}, \mathbf{m}, \mathbf{n} \times \mathbf{m}\}$ is an orthonormal basis consisting of linearly independent eigenvectors of Q corresponding to the

Received October 06, 2022; Accepted February 24, 2023.
2020 Mathematics Subject Classification: Primary 49T99, 34A34; Secondary 34K18, 49J49.
Key words and phrases: applied field,defects, landau-de Gennes, liquid crystals.
This work was financially supported by research fund of Chungnam National University in 2018 .

eigenvalues

$$\frac{1}{3}(2S_1 - S_2),\ -\frac{1}{3}(S_1 + S_2),\ \frac{1}{3}(2S_2 - S_1).$$

In the isotropic phase, Q becomes zero. We say that a liquid crystal is uniaxial if two eigenvalues of Q are equal, and it is biaxial when three eigenvalues of Q are distinct. In the uniaxial nematic phase, the order tensor Q can be written as

$$Q = S(\mathbf{n} \otimes \mathbf{n} - \frac{1}{3}I), \tag{1.1}$$

where S is real and $\mathbf{n}$ is a unit vector in $\mathbf{R}^3$. It can be also shown that

$$\beta^2 = 1 - \frac{6[tr(Q^3)]^2}{[tr(Q^2)]^3},$$

is in (0.1] if and only if Q is in a biaxial nematic phase. When Q is uniaxial, then β^2 is equal to zero.

Throughout this paper, we assume that $\mathbf{n}$ and $\mathbf{m}$ are perpendicular to $z-$axis. Since Q is symmetric and traceless, Q can be written as

$$Q = \begin{pmatrix} q_1 - \frac{q_3}{2} & q_2 & 0 \\ q_2 & -q_1 - \frac{q_3}{2} & 0 \\ 0 & 0 & q_3 \end{pmatrix} \tag{1.2}$$

In section 2, we address the existence of minimizers for the Landau-de Gennes energy functional. In order to investigate the behaviour of molecular directions, we utilize numerical method to obtain approximated solutions and investigate behaviour of singularities of minimizers with or without applied fields in section 3 and section 4.

2. Existence of minimizers

The Landau-de Gennes energy functional of nematic liquid crystal we consider is given by

$$\mathcal{E}(Q) = \int_\Omega \{F_{el}(\nabla Q) + F_b(Q) + f_{elec}(Q, \mathbf{E})\} d\mathbf{x}. \tag{2.1}$$

The elastic energy density F_{el} and bulk energy density F_b are given by

$$F_{el} = \frac{L_1}{2}|\nabla Q|^2 + \frac{L_3}{2}|\nabla \times Q|^2,$$
$$F_b = \frac{a}{2}trQ^2 - \frac{b}{3}(trQ^3) + \frac{c}{4}(trQ^2)^2$$

Here L_1 and L_3 are independent elastic constants, and $a = A_0(T - T^*)$, where T^* is nematic super-cooling temperature and $A_0 > 0$, $b > 0$, $c > 0$ are constants depending on the material.

We assume that the temperature dependent constant a is negative, so that the bulk energy density F_b attains its global minimum at $S^+ = \frac{b+\sqrt{b^2-24ac}}{4c}$, and has local minimum at $S^- = \frac{b-\sqrt{b^2-24ac}}{4c}$(see [1]). We also consider Dirichlet boundary conditions on the inner boundary $\partial\Omega_{in}$ and outer boundary $\partial\Omega_{out}$ such that

$$Q = S^+(\mathbf{n}_0 \otimes \mathbf{n}_0 - \frac{1}{3}I), \text{ on } \partial\Omega, \tag{2.2}$$

where $\mathbf{n}_0 : \partial\Omega \to \mathbb{S}^2$ is given by $\mathbf{n}_0 = \mathbf{n}_{in}$ on $\partial\Omega_{in}$ and $\mathbf{n}_0 = \mathbf{n}_{out}$ on $\partial\Omega_{out}$ with $\mathbf{n}_{in}$ and $\mathbf{n}_{out}$ being fixed unit vector fields on $\partial\Omega_{in}$ and $\partial\Omega_{out}$ respectively.

The free energy $\mathcal{E}_{elec}$ associated with electric field is given by

$$\begin{aligned} \mathcal{E}_{elec} &= -\int_\Omega \frac{1}{2}\mathbf{E}\cdot\mathbf{D}d\mathbf{x}, \\ \mathbf{D} &= (\varepsilon_a I + \varepsilon_\perp Q)\mathbf{E}, \end{aligned}$$

where ε_a and $\varepsilon_\perp$ are the isotropic and anisotropic dielectric permittivities, respectively. By Maxwell's equations, we assume that $\mathbf{E} = -\nabla\psi$, for some scalar potential function ψ and $\mathbf{D}$ satisfies

$$\nabla\cdot\mathbf{D} = 0. \tag{2.3}$$

Given a scalar function ψ_0 on $\partial\Omega$, we impose it as a boundary condition for ψ to obtain

$$\begin{cases} -\nabla\cdot(\varepsilon_a I + \varepsilon_\perp Q)(\nabla\psi)) = 0, & \text{in } \Omega, \\ \psi = \psi_0, & \text{on } \partial\Omega. \end{cases}$$

Taking a special form Q in (1.2) into (2.1), we obtain a new energy functional in terms of $\mathbf{q} = (q_1, q_2, q_3)$ by abuse of notation as follows:

$$\mathcal{E}(\mathbf{q},\psi) := \mathcal{E}(Q,\psi) = \int_\Omega \{F_{el}(\nabla\mathbf{q}) + F_b(\mathbf{q}) + f_{elec}(\mathbf{q},\psi)\}d\mathbf{x}. \tag{2.4}$$

where

$$
\begin{aligned}
F_{el}(\nabla \mathbf{q}) &= F_1(\nabla \mathbf{q}) + F_2(\nabla \mathbf{q}) \\
F_1(\nabla \mathbf{q}) &= (L_1 + \frac{L_3}{2})\nabla q_1 \cdot \nabla q_1 + (L_1 + \frac{L_3}{2})\nabla q_2 \cdot \nabla q_2 + (\frac{3}{4}L_1 + \frac{5}{8}L_3)\nabla q_3 \cdot \nabla q_3 \\
F_2(\nabla \mathbf{q}) &= L_3(\partial_x q_1 \partial_y q_2 - \partial_y q_1 \partial_x q_2 + \frac{1}{2}\partial_x q_2 \partial_y q_3 + \frac{1}{2}\partial_y q_2 \partial_x q_3 + \frac{1}{2}\partial_x q_1 \partial_x q_3 - \frac{1}{2}\partial_y q_1 \partial_y q_3) \\
F_b(\mathbf{q}) &= a(q_1^2 + q_2^2 + \frac{3}{4}q_3^2) - b(\frac{1}{4}q_3^3 - q_3 q_1^2 - q_3 q_2^2) + c(q_1^2 + q_2^2 + \frac{3}{4}q_3^2)^2 \\
f_{elec}(\mathbf{q}, \psi) &= -\frac{1}{2}\varepsilon_a \nabla\psi \cdot \nabla\psi - \frac{1}{2}\varepsilon_\perp \bigg(q_1(\psi_x^2 - \psi_y^2) + 2q_2\psi_x\psi_y - q_3(\frac{1}{2}\psi_x^2 + \frac{1}{2}\psi_y^2 - \psi_z^2) \bigg).
\end{aligned}
$$

We now define the admissible spaces as

$$
\begin{aligned}
\mathcal{X} &= \{\mathbf{q} \in H^1(\Omega; \mathbf{R}^3) |\ \mathbf{q} = \mathbf{q}_0 \text{ on } \partial\Omega\}, \\
\mathcal{Y} &= \{\psi \in H^1(\Omega) : \psi = \psi_0 \text{ on } \partial\Omega\}, \\
\mathcal{H} &= \mathcal{X} \times \mathcal{Y},
\end{aligned}
$$

where $\mathbf{q}_0$ is determined by $\mathbf{n}_0$ in (2.2), and $H^1(\Omega)$ and $H^1(\Omega, \mathbf{R}^3)$ are Sobolev spaces [4]. In the following, we prove the existence of minimizers for $\mathcal{E}$ in $\mathcal{H}$.

THEOREM 2.1. *Suppose that $L_1 > 0$ and $3L_1 + 4L_3 > 0$. Then there exists a $(\bar{q}, \bar{\psi}) \in \mathcal{H}$ such that*

$$
\mathcal{E}(\bar{q}, \bar{\psi}) = \inf_{q \in \mathcal{H}} \mathcal{E}(q, \psi),
$$

Proof. Let

$$
\mathcal{W}(\mathbf{q}) = \int_\Omega \{F_{el}(\nabla \mathbf{q}) + F_b(\mathbf{q})\} d\mathbf{x}.
$$

In the spirit of the proof given in [2], it suffices to prove that $\mathcal{W}$ has a minimizer in $\mathcal{X}$. Given $\mathbf{q}(\mathbf{x})$ for $\mathbf{x} = (x, y) \in \Omega$, we define $\mathbf{p}(\mathbf{x}) \in \mathbf{R}^6$ by

$$
\mathbf{p}(\mathbf{x}) = (\partial_x q_1(\mathbf{x}), \partial_y q_1(\mathbf{x}), \partial_x q_2(\mathbf{x}), \partial_y q_2(\mathbf{x}), \partial_x q_3(\mathbf{x}), \partial_y q_3(\mathbf{x}))^T.
$$

Let

$$
B = \begin{pmatrix}
L_1 + \frac{L_3}{2} & 0 & 0 & \frac{L_3}{2} & \frac{L_3}{4} & 0 \\
0 & L_1 + \frac{L_3}{2} & -\frac{L_3}{2} & 0 & 0 & -\frac{L_3}{4} \\
0 & -\frac{L_3}{2} & L_1 + \frac{L_3}{2} & 0 & 0 & \frac{L_3}{4} \\
\frac{L_3}{2} & 0 & 0 & L_1 + \frac{L_3}{2} & \frac{L_3}{4} & 0 \\
\frac{L_3}{4} & 0 & 0 & \frac{L_3}{4} & \frac{3}{4}L_1 + \frac{5}{8}L_3 & 0 \\
0 & -\frac{L_3}{4} & \frac{L_3}{4} & 0 & 0 & \frac{3}{4}L_1 + \frac{5}{8}L_3.
\end{pmatrix}
$$

It can be seen by calculations that the eigenvalues $\{\lambda_i\}_{i=1}^6$ of the matrix B are given by

$$\begin{cases} \lambda_1 = \lambda_2 = L_1, \\ \lambda_3 = \lambda_4 = \frac{7}{8}L_1 + \frac{13}{16}L_3 - \frac{\sqrt{4L_1^2+12L_1L_3+41L_3^2}}{16}, \\ \lambda_5 = \lambda_6 = \frac{7}{8}L_1 + \frac{13}{16}L_3 + \frac{\sqrt{4L_1^2+12L_1L_3+41L_3^2}}{16}. \end{cases}$$

It is easy to show that $\lambda_i > 0$, for $i = 1, 2, \cdots, 6$. Since B is symmetric, there exists an orthonormal matrix $\mathcal{O}$ such that $\mathcal{O}^T B\mathcal{O}$ is a diagonal matrix whose entries are $\{\lambda_i\}_{i=1}^6$. Then for $\mathbf{p} \neq 0$, we have

$$\begin{aligned} F_{el}(\nabla \mathbf{q}) =& \mathbf{p}^T\mathcal{O}^T B\mathcal{O}\mathbf{p} = \sum_{i=1}^{6} \lambda_i v_i^2 \\ \geq& \lambda|\mathcal{O}\mathbf{p}|^2 = \lambda|\mathbf{p}|^2 = \lambda|\nabla \mathbf{q}|^2, \end{aligned}$$

where $(v_1, v_2, ..., v_6)^T = \mathcal{O}\mathbf{p}$ and $\lambda = \min\{\lambda_1, \lambda_2, \cdots, \lambda_6\}$. This implies that $\mathcal{W}$ is coercive. By the direct method in the calculus of variations, one see that $\mathcal{W}$ achieves its minimum in $\mathcal{X}$. For the existence of minimizers for $\mathcal{E}$ on $\mathcal{H}$, we refer the reader to [2]. □

3. The Euler-Lagrange equations and the radial external electric field

In this section, we discuss the Euler-Lagrange equations corresponding to $\mathcal{E}$ discussed in the previous section. We also introduce a radially symmetric external field in order to investigate how singularities for solutions response to applied fields.

The external electric field we consider is given by

$$\mathbf{E}(\mathbf{x}) = C_e \frac{\mathbf{x}}{|\mathbf{x}|^2} = \frac{C_e}{\rho}\mathbf{e}_\rho, \mathbf{x} \in \Omega,$$

where $\rho = |\mathbf{x}|, \mathbf{e}_\rho = \frac{\mathbf{x}}{|\mathbf{x}|}$, and C_e is a fixed constant. Notice that s is the radius of outer circle for $\Omega = B_s \backslash B_\ell$. We introduce scalings as below:

$$\tilde{\mathbf{x}} = \frac{\mathbf{x}}{s}, \quad \tilde{\ell} = \frac{\ell}{s}, \quad \tilde{\Omega} = \{\tilde{x} | s\tilde{x} \in \Omega\}.$$

For $\tilde{x} \in \tilde{\Omega}$, we define $\tilde{\mathbf{q}}$ and $\tilde{\mathcal{E}}$ by

$$\tilde{\mathbf{q}}(\tilde{\mathbf{x}}) = (\tilde{q}_1(\tilde{\mathbf{x}}), \tilde{q}_2(\tilde{\mathbf{x}}), \tilde{q}_3(\tilde{\mathbf{x}})) = \frac{\sqrt{2}c}{b}(q_1(s\tilde{\mathbf{x}}), q_2(s\tilde{\mathbf{x}}), \sqrt{3}q_3(s\tilde{\mathbf{x}})/2),$$
$$\tilde{\mathcal{E}}(\tilde{\mathbf{q}}) = \frac{c^2}{Lb^2}\mathcal{E}(\mathbf{q}).$$

After dropping the tildes, we have $\Omega = B_1 \backslash B_\ell (0 < \ell < 1)$ and the energy (2.4) reduces to

$$\mathcal{E}(\mathbf{q}) = \mathcal{E}_{el}(\nabla \mathbf{q}) + \mathcal{E}_b(\mathbf{q}) + \mathcal{E}_{elec}(\mathbf{q}), \tag{3.1}$$

where

$$\begin{aligned}
\mathcal{E}_{el}(\nabla \mathbf{q}) &= \mathcal{E}_1(\nabla \mathbf{q}) + \mathcal{E}_2(\nabla \mathbf{q}) \\
\mathcal{E}_1(\nabla \mathbf{q}) &= \int_\Omega \Big[\frac{K_1}{2}(\nabla q_1 \cdot \nabla q_1 + \nabla q_2 \cdot \nabla q_2 + \nabla q_3 \cdot \nabla q_3) \\
&\quad + \frac{K_3}{4}(\nabla q_1 \cdot \nabla q_1 + \nabla q_2 \cdot \nabla q_2 + \frac{5}{3}\nabla q_3 \cdot \nabla q_3) \Big] d\mathbf{x}, \\
\mathcal{E}_2(\nabla \mathbf{q}) &= \int_\Omega \frac{K_3}{2}\Big(\frac{\partial q_1}{\partial x}\frac{\partial q_2}{\partial y} - \frac{\partial q_2}{\partial x}\frac{\partial q_1}{\partial y} + \frac{1}{\sqrt{3}}\frac{\partial q_3}{\partial x}\frac{\partial q_1}{\partial x} + \frac{1}{\sqrt{3}}\frac{\partial q_2}{\partial y}\frac{\partial q_3}{\partial x} \\
&\quad + \frac{1}{\sqrt{3}}\frac{\partial q_2}{\partial x}\frac{\partial q_3}{\partial y} - \frac{1}{\sqrt{3}}\frac{\partial q_1}{\partial y}\frac{\partial q_3}{\partial y}\Big) d\mathbf{x}, \\
\mathcal{E}_b(\mathbf{q}) &= \int_\Omega \Big[\frac{1}{\varepsilon^2}\Big[\frac{T_a}{2}(q_1^2 + q_2^2 + q_3^2) - \frac{1}{\sqrt{6}}(\frac{q_3^3}{3} - q_3 q_1^2 - q_3 q_2^2) + \frac{1}{4}(q_1^2 + q_2^2 + q_3^2)^2\Big] \Big] d\mathbf{x}, \\
\mathcal{E}_{elec}(\mathbf{q}) &= \int_\Omega \Big[-sgn(\varepsilon_a)\frac{C_e^2}{|\mathbf{x}|^2} - sgn(\varepsilon_a)\frac{\sqrt{2}\tilde{\varepsilon}C_e^2}{2|\mathbf{x}|^2}\Big(q_1\frac{x^2 - y^2}{|\mathbf{x}|^2} + q_2\frac{2xy}{|\mathbf{x}|^2} - \frac{q_3}{\sqrt{3}}\Big) \Big] d\mathbf{x},
\end{aligned}$$

where $L = \max\{|L_1|, |L_3|\}$, $K_1 = \frac{L_1}{L}$, $K_3 = \frac{L_3}{L}$, $\frac{1}{\varepsilon^2} = \frac{s^2 b^2}{Lc}$, $T_a = \frac{ac}{b^2}$, $\tilde{C}_e = \frac{c}{b}\sqrt{\frac{|\varepsilon_a|}{2L}}C_e$, and $\tilde{\varepsilon} = \frac{b\varepsilon_\perp}{c\varepsilon_a}$.

The Euler-Lagrange equations corresponding to (3.1) are given by

$$\begin{cases}
-(K_1 + \frac{K_3}{2})\Delta q_1 - \frac{K_3}{2\sqrt{3}}(\frac{\partial^2 q_3}{\partial x^2} - \frac{\partial^2 q_3}{\partial y^2}) - sgn(\varepsilon_a)\frac{\sqrt{2}\tilde{\varepsilon}C_e^2}{2|\mathbf{x}|^2}\frac{x^2 - y^2}{|\mathbf{x}|^2} \\
+\frac{1}{\varepsilon^2}\Big[T_a q_1 + \frac{2}{\sqrt{6}}q_3 q_1 + q_1(q_1^2 + q_2^2 + q_3^2)\Big] = 0, \text{in } \Omega \\
-(K_1 + \frac{K_3}{2})\Delta q_2 - \frac{K_3}{2\sqrt{3}}(2\frac{\partial^2 q_3}{\partial x \partial y}) - sgn(\varepsilon_a)\frac{\sqrt{2}\tilde{\varepsilon}C_e^2}{|\mathbf{x}|^2}\frac{xy}{|\mathbf{x}|^2} \\
+\frac{1}{\varepsilon^2}\Big[T_a q_2 + \frac{2}{\sqrt{6}}q_3 q_2 + q_2(q_1^2 + q_2^2 + q_3^2)\Big] = 0, \text{in } \Omega \\
-(K_1 + \frac{5K_3}{6})\Delta q_3 - \frac{K_3}{2\sqrt{3}}(\frac{\partial^2 q_1}{\partial x^2} - \frac{\partial^2 q_1}{\partial y^2} + 2\frac{\partial^2 q_2}{\partial x \partial y}) + sgn(\varepsilon_a)\frac{\tilde{\varepsilon}C_e^2}{\sqrt{6}|\mathbf{x}|^2} \\
+\frac{1}{\varepsilon^2}\Big[T_a q_3 + \frac{1}{\sqrt{6}}(q_1^2 + q_2^2 - q_3^2) + q_3(q_1^2 + q_2^2 + q_3^2)\Big] = 0, \text{in } \Omega.
\end{cases} \tag{3.2}$$

For the boundary condition $\mathbf{q} = (q_1, q_2, q_3)$, it is satisfied that

$$\begin{cases} q_1 = \frac{\sqrt{2}c}{b} S^+ (n_1^2 - \frac{1}{2}), \\ q_2 = \frac{\sqrt{2}c}{b} S^+ n_1 n_2, \\ q_3 = -\frac{\sqrt{6}c}{6b} S^+, \qquad \text{on } \partial\Omega_{out}, \end{cases} \tag{3.3}$$

and

$$\begin{cases} q_1 = \frac{\sqrt{2}c}{b} S^+ (m_1^2 - \frac{1}{2}), \\ q_2 = \frac{\sqrt{2}c}{b} S^+ m_1 m_2, \\ q_3 = -\frac{\sqrt{6}c}{6b} S^+, \qquad \text{on } \partial\Omega_{in}. \end{cases} \tag{3.4}$$

where (n_1, n_1) and (m_1, m_2) are given unit vectors and S^+ is introduced in section 2.

4. Results of computational experiments

In this section, we study solutions to the Euler-Lagrange equations (3.2) by way of a numerical method developed in [3]. First, choose C_0 such that

$$\mathcal{E}_N(\mathbf{q}) := \mathcal{E}(\mathbf{q}) + C_0 > 0, \tag{4.1}$$

for all $\mathbf{q}$. Such a constant C_0 exists because $\mathcal{E}$ is bounded from below. The general form of gradient flow is given by

$$\begin{aligned} \frac{\partial \mathbf{q}}{\partial t} &= -\mu, \\ \mu = \frac{\delta \mathcal{E}_N}{\delta \mathbf{q}} &= \frac{\delta \mathcal{E}_1}{\delta \mathbf{q}} + \frac{\delta \mathcal{E}_2}{\delta \mathbf{q}} + \frac{\delta \mathcal{E}_{elec}}{\delta \mathbf{q}} + \frac{\delta \mathcal{E}_b}{\delta \mathbf{q}}. \end{aligned}$$

We adopt the SAV method studied in [3] to our system. Let

$$\gamma(t) = \mathcal{E}_N(\mathbf{q}(t)), \text{ for } t > 0.$$

Then it is easy to check that

$$\frac{d\gamma(t)}{dt} = \frac{d\mathcal{E}_N(\mathbf{q})}{dt} = \int_\Omega \frac{\delta \mathcal{E}_N}{\delta \mathbf{q}} \frac{\partial \mathbf{q}}{\partial t} d\mathbf{x} = -(\mu, \mu) \leq 0.$$

Define $\xi(t) = \gamma(t)/\mathcal{E}_N(\mathbf{q}(t))$. The first-order scheme of SAV is given by

$$\begin{cases} \frac{\mathbf{q}^{n+1}-\eta^{n+1}\mathbf{q}^n}{\Delta t} = -\mu^{n+1} \\ \mu^{n+1} = \frac{\delta \mathcal{E}_1}{\delta \mathbf{q}}(\mathbf{q}^{n+1}) + \eta^{n+1}(\frac{\delta \mathcal{E}_2}{\delta \mathbf{q}}(\mathbf{q}^n) + \frac{\delta \mathcal{E}_{elec}}{\delta \mathbf{q}}(\mathbf{q}^n) + \frac{\delta \mathcal{E}_b}{\delta \mathbf{q}}(\mathbf{q}^n)) \\ \xi^{n+1} = \frac{\gamma^{n+1}}{\mathcal{E}_N(\bar{\mathbf{q}}^{n+1})} \\ \frac{\gamma^{n+1}-\gamma^n}{\Delta t} = -\xi^{n+1}(\bar{\mu}^{n+1}, \bar{\mu}^{n+1}) \\ \eta^{n+1} = 1 - (1-\xi^{n+1})^2 \\ \bar{\mathbf{q}}^{n+1} = \mathbf{q}^{n+1}/\eta^{n+1} \\ \bar{\mu}^{n+1} = \frac{\delta \mathcal{E}_1}{\delta \mathbf{q}}(\bar{\mathbf{q}}^{n+1}) + \frac{\delta \mathcal{E}_2}{\delta \mathbf{q}}(\bar{\mathbf{q}}^{n+1}) + \frac{\delta \mathcal{E}_{elec}}{\delta \mathbf{q}}(\bar{\mathbf{q}}^{n+1}) + \frac{\delta \mathcal{E}_b}{\delta \mathbf{q}}(\bar{\mathbf{q}}^{n+1}). \end{cases}$$

For a boundary condition for Q on $\partial\Omega$, we take

$$Q = S^+(\mathbf{n}_0 \otimes \mathbf{n}_0 - \frac{1}{3}I),$$

where for $\theta \in [0, 2\pi]$,

$$\mathbf{n}_0(\mathbf{x}) = \begin{cases} (-\sin\frac{k_{in}\theta}{2}, \cos\frac{k_{in}\theta}{2}, 0) & \text{if } \mathbf{x} = (\ell\cos\theta, \ell\sin\theta) \in \partial\Omega_{in}, \\ (\cos\frac{k_{out}\theta}{2}, \sin\frac{k_{out}\theta}{2}, 0) & \text{if } \mathbf{x} = (\cos\theta, \sin\theta) \in \partial\Omega_{out}. \end{cases} \tag{4.2}$$

For the boundary condition $\mathbf{q}$ on $\partial\Omega$, we obtain that for $\theta \in [0, 2\pi]$, $\mathbf{q} = (q_1, q_2, q_3)$ satisfies

$$\begin{cases} q_1(\ell\cos\theta, \ell\sin\theta) = -\frac{\sqrt{2}}{8}(1 + \sqrt{1-24T_a})\cos k_{in}\theta, \\ q_2(\ell\cos\theta, \ell\sin\theta) = -\frac{\sqrt{2}}{8}(1 + \sqrt{1-24T_a})\sin k_{in}\theta, \\ q_3(\ell\cos\theta, \ell\sin\theta) = -\frac{\sqrt{6}}{24}(1 + \sqrt{1-24T_a}), \end{cases} \quad \text{on } \partial\Omega_{in}$$

and

$$\begin{cases} q_1(\cos\theta, \sin\theta) = \frac{\sqrt{2}}{8}(1 + \sqrt{1-24T_a})\cos k_{out}\theta, \\ q_2(\cos\theta, \sin\theta) = \frac{\sqrt{2}}{8}(1 + \sqrt{1-24T_a})\sin k_{out}\theta, \\ q_3(\cos\theta, \sin\theta) = -\frac{\sqrt{6}}{24}(1 + \sqrt{1-24T_a}), \end{cases} \quad \text{on } \partial\Omega_{out}.$$

The molecular direction is represented by the eigenvector corresponding to the largest eigenvalue of Q. On the boundary, $\mathbf{n}_0$ is the directions of molecule and its topological degrees are $k_{in}/2$ and $k_{out}/2$ on inner and outer boundaries respectively. We set $K_1 = 1$, $K_3 = 0.5$, $\varepsilon = 0.01$, $\ell = 0.1$, $T_a = -0.1$, $\tilde{\varepsilon} = 1.5$, $\varepsilon_a > 0$. For each run, we set $\Delta t = 0.0001$, and carry out the simulation over the time interval $0 \le t \le 1$.

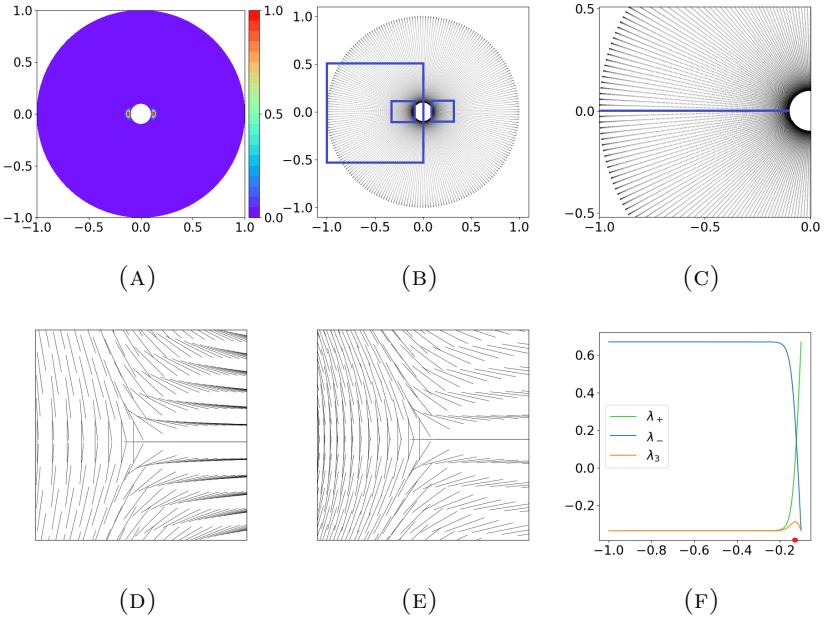

FIGURE 1. (A)values of β^2 in the domain Ω, (C),(D),(E): molecular direction field in the region magnified from boxed regions in (B) from the left to the right, (F): three eigenvalues of Q along the blue line specified in (C). $C_e = 0$, $k_{in} = 3$, $k_{out} = 1$ were taken in simulations.

4.1. Without an applied field

We carried out numerical simulation without an applied field so as to understand behavior of molecules in the system. We first take $k_{in} = 3, k_{out} = 1$. Computation results are shown in Figure 1. In Figure 1, values of β^2 which is biaxial parameter are described in (A). One may see from (A) in Figure 1 that molecules are uniaxial(purple color) for the most part of the region although there exist two small regions(red color) close to inner boundary for biaxial nematic state. These two biaxial regions are located near inner boundary and symmetric with respect to $y-$axis. In order to understand directions of molecules, we magnify two parts of region(boxed regions) in (B) including a singularity and display them in (D) and (E). The picture (D) which is a magnified region near left singular point indicates that the topological degree of the singular point is $-\frac{1}{2}$. The topological degree of a singular point located on the

right is also $-\frac{1}{2}$ as shown in the picture (E). Three eigenvalues of the order tensor Q for the line specified in (C) are shown in (F). We see that two eigenvalues are crossed at the singular point and molecule at the singular point(defect core) is uniaxial.

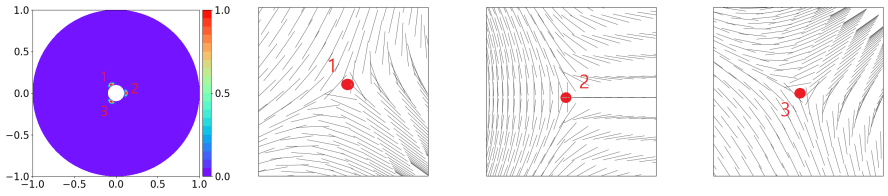

(A) (B) (C) (D)

FIGURE 2. (A)values of β^2 in the domain Ω, (C) is magnified from the big box in (B) , (D) and (E): molecular direction field in the region magnified from two small boxed regions in (B) from the left to the right. For simulations, we take $C_e = 0$, $k_{in} = 4$, $k_{out} = 1$.

In Figure 2, we display computational results when $k_{in} = 4,\ k_{out} = 1$. In this case, the total topological degree of molecular direction on the boundary of Ω is $-3/2$, and our simulation shows that there are three singular points whose topological degrees are $-1/2$ near them as shown in (B), (C) and (D). Defects are located at points which are threefold symmetric with the angle $\frac{2\pi}{3}$ and defect cores are also uniaxial. In order to study behavior of defects with respect to constants k_{in} and k_{out}, we performed our method several times with different values and the results are shown in Table 1.

	Degrees of defects	Degree on $\partial\Omega_{in}$	Degree on $\partial\Omega_{out}$
$k_{in} = 1, k_{out} = 1$	$-\frac{1}{2}, +\frac{1}{2}$	$+\frac{1}{2}$	$+\frac{1}{2}$
$k_{in} = 1, k_{out} = 2$	$+\frac{1}{2}$	$+\frac{1}{2}$	$+1$
$k_{in} = 1, k_{out} = 3$	$+\frac{1}{2}, +\frac{1}{2}$	$+\frac{1}{2}$	$+\frac{3}{2}$
$k_{in} = 1, k_{out} = 4$	$+\frac{1}{2}, +\frac{1}{2}, +\frac{1}{2}$	$+\frac{1}{2}$	$+2$
$k_{in} = 2, k_{out} = 1$	$-\frac{1}{2}$	$+1$	$+\frac{1}{2}$
$k_{in} = 3, k_{out} = 1$	$-\frac{1}{2}, -\frac{1}{2}$	$+\frac{3}{2}$	$+\frac{1}{2}$
$k_{in} = 4, k_{out} = 1$	$-\frac{1}{2}, -\frac{1}{2}, -\frac{1}{2}$	$+2$	$+\frac{1}{2}$

TABLE 1. Degrees of defects

If $k_{in} = 1$ and $k_{out} = 1$, then the total topological degree of direction field on the boundary $\partial\Omega$ becomes 0. In this case, two defects appear in the domain with their local topological degree being $\frac{1}{2}$ and $-\frac{1}{2}$. For other cases, we refer the reader to Table 1.

4.2. With an applied field

We now try to investigate how an applied field has an effect on defects. In order to do so, we fix $k_{in} = 3$, $k_{out} = 1$ and increase constant C_e(strength of voltage) from 0 to 2. The computation results with $C_e = 2$ are shown in Figure 3. From (A) in Figure 3, we can see that molecules are also uniaxial(purple color) for the most part of region and there exist two small biaxial regions(red color). But compared to the results without an electric field, these two biaxial regions appear to be moved to the left as shown in (A) due to the interaction with the radial applied field.

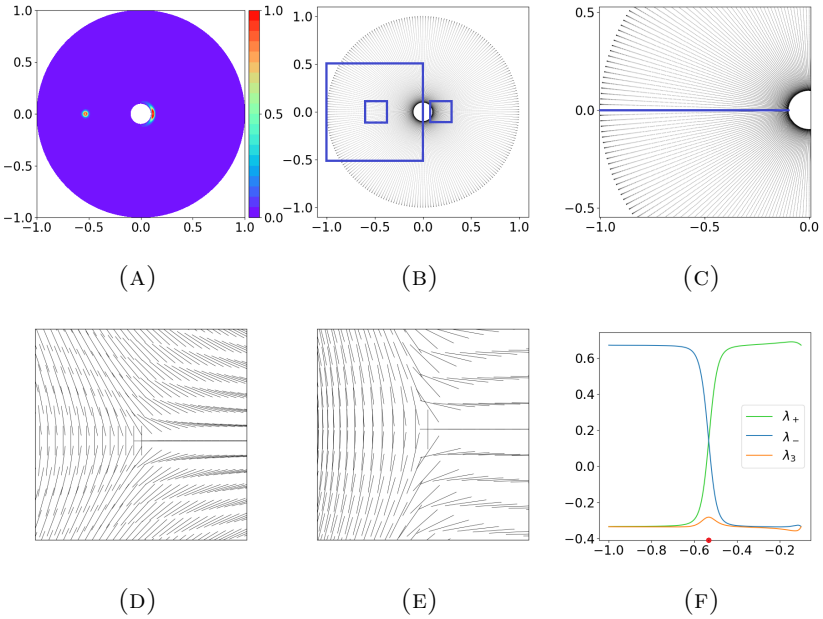

FIGURE 3. (A)values of β^2 in the domain Ω, (C) is magnified from the big box in (B) , (D) and (E): molecular direction field in the region magnified from two small boxed regions in (B) from the left to the right, (F): three eigenvalues of Q along the blue line in (C). $C_e = 2$, $k_{in} = 3$, $k_{out} = 1$ were used for simulations.

In order to understand the effect of the strength C_e of the applied field, we track down locations of defect cores when C_e is increased from 0 to 2. As shown in Table 2, we observe that defect cores are shifted to the left when we increase the strength of the applied field.

	Degree	position (ρ, θ)	Degree	position (ρ, θ)
$C_e = 0$	$-\frac{1}{2}$	$(0.1214, \pi)$	$-\frac{1}{2}$	$(0.1214, 0)$
$C_e = 1$	$-\frac{1}{2}$	$(0.1276, \pi)$	$-\frac{1}{2}$	$(0.1195, 0)$
$C_e = 2$	$-\frac{1}{2}$	$(0.5342, \pi)$	$-\frac{1}{2}$	$(0.1160, 0)$

TABLE 2. Degrees and coordinate position of defects

Next, we discuss how molecular directions deviate from the radial applied field. In order to do so, we introduce a variable α which measures the angle between the applied field and molecular direction as

$$\alpha = |\mathbf{n} \cdot e_\rho|.$$

In Figure 4, values of α for simulation results with $C_e = 0, 1, 2$ are described in different colors. In the blue colored region, molecules are perpendicular to the direction of the radial applied filed and molecules are aligned parallel to the direction of the applied field in red colored region. We also see that the red colored region gets larger when the strength of the applied field is increased.

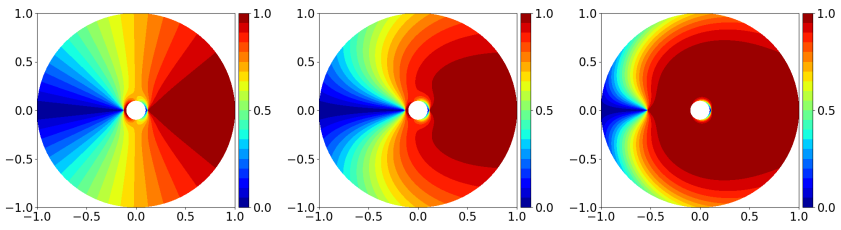

(A) (B) (C)

FIGURE 4. The parameter α with various C_e, (A):$C_e = 0$, (B):$C_e = 1$, (C):$C_e = 2$ with $k_{in} = 3, k_{out} = 1$.

5. Conclusion

We introduced the Landau-de Gennes energy functional and radial external field and proved existence of a minimizer for the energy functional on a Sobolev space. With and without an applied field, we investigated behaviour of defects(singularities) of solutions to the corresponding Euler-Lagrange equations by way of a numerical algorithm. In this paper, we did not explain details about the numerical algorithm we used. The details of the algorithm will appear in our forthcoming paper.

References

[1] A. Majumdar and A. Zarnescu. *Landau–de gennes theory of nematic liquid crystals: the oseen–frank limit and beyond.* Arch. Ration. Mech. Anal., **196** (2010), no. 1, 227–280.
[2] J. Park and M. C. Calderer. *Analysis of nonlocal electrostatic effects in chiral smectic c liquid crystals.* SIAM J. Appl. Math., **66** (2006), no. 6, 2107–2126.
[3] F. Huang, et al. *A highly efficient and accurate new scalar auxiliary variable approach for gradient flows.* SIAM J. Sci. Comput., **42** (2020), no. 4, A2514–A2536.
[4] L. C. Evans. *Partial differential equations*, J. Amer. Math. Soc., **19** (2010)
[5] N. J. Mottram and C. Newton. *Introduction to Q-tensor theory.* University of Strathclyde, Department of Mathematics Research Report, 10, 2004.

Jinhae Park
Department of Mathematics
Chungnam National University
99 Daehak-Ro, Yuseong-Gu
Daejeon 34134, Republic of Korea
E-mail: jhpark2003@cnu.ac.kr

He Jin
Department of Mathematics
Chungnam National University
99 Daehak-Ro, Yuseong-Gu
Daejeon 34134, Republic of Korea
E-mail: jinhe5713@gmail.com